Apparatus for endoscopical, laser-based determination of Ciliary Beat Frequency

N. Bogdanović, J. Rička, M. Frenz, H. Walt*, B. Kratiger**

Institut für Angewandte Physik, Universität Bern, Schweiz
*Klinik und Poliklinik für Gynäkologie, Medizinische fakultät, Universität Zurich, Schweiz
**Storz Endoscop Productions GmbH, Schaffhausen, Schweiz

Abstract

Cilia are hair-like protrusions, about 10 µm long, emerging from the epithelium of the bronchial tract and other parts of the body. Their synchronized oscillation of about 10-30 Hz, causes directed transport of surrounding mucosal fluids and adhering micro-particles. Defects in ciliary motility, such as the Primary Ciliary Dyskinesia, are connected to a number of clinical symptoms. Therefore, there is a considerable interest in minimal invasive *in vivo* detection of ciliary beat frequency in the respiratory tract. Previous attempts failed because of lack of the contrast and because of disturbances resulting from the inevitable movements of the probe with respect to the observed surface. We have shown that both problems can be overcome by the technique of *video-endoscopic dynamic speckle interferometry*. The setup, currently employed for the optimization of the design of a clinical prototype, is shown in Fig. 1. Basic principle of the method is shown in Fig. 2. The internal surface of the excised trachea is illuminated with a near infrared laser at 800nm. Diffuse reflection from the epithelium is observed through an imaging fiber bundle. Mixing of the field contributions from the individual fibers generates a speckle field, whose dynamics we record with a high speed CCD camera.

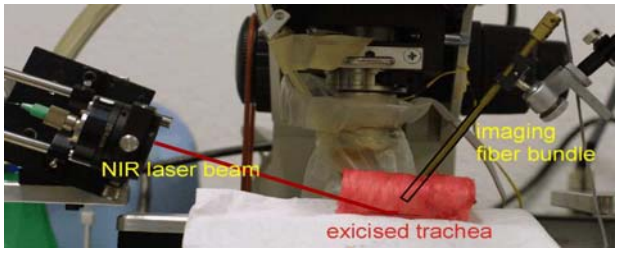

Figure 1. Test Set-up

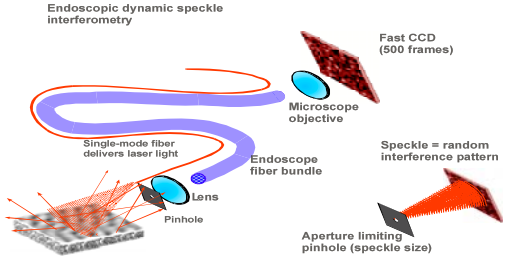

Figure 2. Principle video-endoscopic dynamic speckle interferometry

Laser speckle

The contrast and the resolution of conventional endoscopy is entirely insufficient for direct observation of the ciliary activity (Fig. 3 left). However, any seemingly contrastles, but diffusely scattering surface can be visualized by coherent illumination with a laser: we exploit the formation of speckle pattern (Fig. 3 right). When diffuse objects are illuminated with laser light a characteristic granular pattern is seen. This effect is called speckle. Figure 2 illustrate the principle of a speckle interferometric experiment.

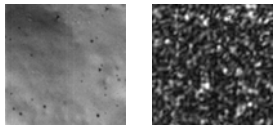

Figure 3. Image of tissue with poor contrast and speckle pattern obtained from same spot

Post-bundle optical mixing Set-up

Two approaches for merging speckle interferometry with fiber-optic endoscopy were tested. In a first approach, one restricts the observation aperture by a pinhole and forms the speckles on the front face of the imaging bundle (Fig. 2). However, contemporate imaging fiber bundles, exhibiting small diameters of individual fibers, offer an interesting alternative to the traditional speckle generation by pinholes: at a wavelength that sufficiently large in comparison with the diameter of the individual fibers, one enters the *single-mode regime*, where a single transversal mode is propagating through each fiber. In this regime, the speckles can be formed after the fiber transmission by superposing the light-fields from a number of fibers by image defocusing. Then the same bundle can be used simultaniously for endoscopic imaging as well as for speckle observation (Fig. 4).

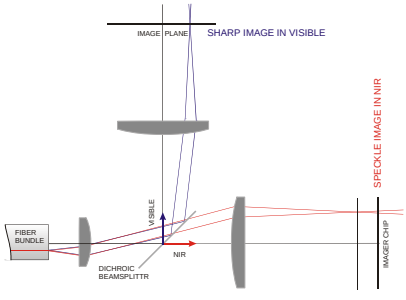

Figure 4. Post bundle optical mixing in combination with endoscopic imaging

Set-up parameters:

Illumination system:
- Laser diode, $\lambda = 780$ nm, $P = 15$ mW

Imaging and speckle forming system:
- Telescopic lens, viewing angle $\alpha = 72.8^{o}$

Endoscopy system:
- Image bundle active area has diameter of $D = 0.8$ mm
- One fiber inside fiber bundle has radius 3.8 µm.
- Distance between fibers inside bundle (center-center) is 6.8 µm

Camera:
- CCD Dalsa CA D1, 500 frames per second, pixel size 16 µm * 16 µm

Principles of speckle analysis

Time series of speckle images can be analyzed in terms of second order statistics - the correlation function. We are interested in spatial as well as temporal properties of the scattering process. The cross-correlation $G_{ij}(\xi,\eta)$ is defined as

$$G_{i,j}(\xi,\eta) = \left\langle F_i(x,y) * F_j(x+\xi, y+\eta) \right\rangle_{x,y}$$

Here, $F_i(x,y)$ and $F_j(x+\xi, y+\eta)$ represents the luminosity distribution in the speckle pattern in the images i, j separated by a time lag (j-i)$\Delta\tau$, as measured at a position shifted by ε, η with respects to x, y in i. Two typical correlogramms are shown in Fig. 5.

The characteristic feature of a correlogramm is a more or less pronounced peak. A shift of the peak position with respect to the origin reflects translational motion of the sample. By tracking the peak position we monitore the relative motion between specimen and detector. The amplitude of the peak represents the degree of time correlation $G(\tau)$. In the presence of synchronized ciliary beat the decorrelation is modulated by CBF beat frequency, Fig. 6. From $G(\tau)$ we obtain by Fourier transformation the desired power spectrum of the beat and/or fluctuations.

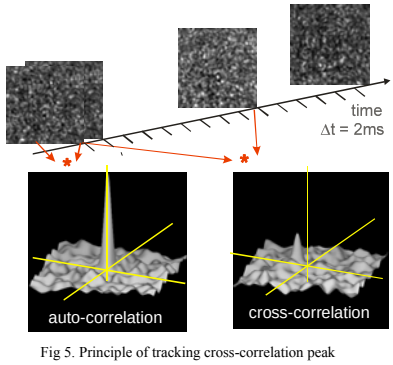

Fig 5. Principle of tracking cross-correlation peak

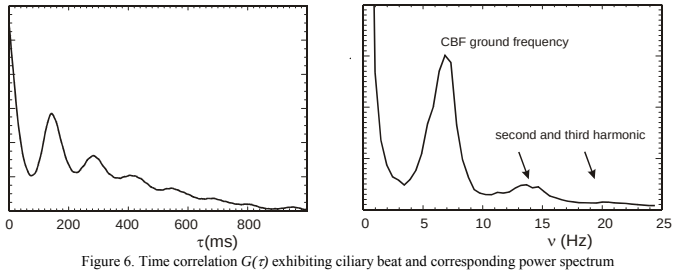

Figure 6. Time correlation $G(\tau)$ exhibiting ciliary beat and corresponding power spectrum

Results

Examples of results obtained from pig and turkey trachea samples are shown in figures 7-11. Figures 7 and 8 show the results from a static, undisturbed sample, measured at a position with well developed mucus transport (as we know from microscopic observations at the same position). The peak in the power spectrum at 9 Hz can be clearly attributed to ciliary beating. Figure 8 shows the trace obtained from speckle tracking. The ciliary beat manifests itself as the small wiggles, whereas the overall displacement most likely reflects the mucus transport.

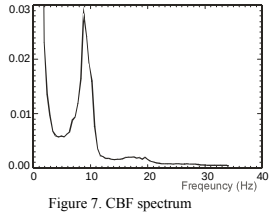

Figure 7. CBF spectrum

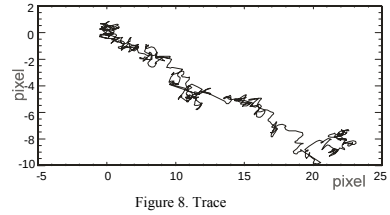

Figure 8. Trace

Figure 9. is an example of rather poor spectrum, measured in the presence of disturbing motion. During this measurement the sample was subject to a jerk, as can be clearly seen in tracing results shown in Fig.10. The tracing information can be used to improve the quality of the spectrum, as is shown in Fig. 11. The procedure was quite simple. We discard the first 300 images poluted by the rapid motion of the sample.

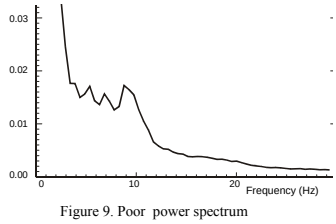

Figure 9. Poor power spectrum

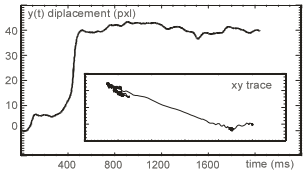

Figure 10. y displacement and xy trace

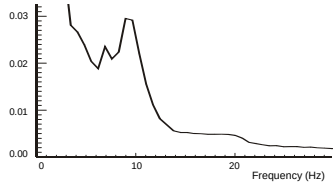

Figure 11. Improved power spectrum

Still to be done

- Develope a laser illuminator providing a nearly collimated beam. The preferred illumination geometry is still near specular reflection.
- Incorporate the setup in a real endoscope.
- Improve and implement the data processing algorithms in a user software.

KTI PROJECT 6146.3